



Minerva Access is the Institutional Repository of The University of Melbourne

Author/s:

Guan, S;Gray, HA;Schache, AG;Feller, J;de Steiger, R;Pandy, MG

Title:

In vivo six-degree-of-freedom knee-joint kinematics in overground and treadmill walking following total knee arthroplasty

Date:

2017-08-01

Citation:

Guan, S., Gray, H. A., Schache, A. G., Feller, J., de Steiger, R. & Pandy, M. G. (2017). In vivo six-degree-of-freedom knee-joint kinematics in overground and treadmill walking following total knee arthroplasty. *Journal of Orthopaedic Research*, 35 (8), pp.1634-1643. <https://doi.org/10.1002/jor.23466>.

Persistent Link:

<https://hdl.handle.net/11343/292112>

21 **Running title.** TKA kinematics in overground walking

22

23 **Author contributions statement.** All authors contributed to this work. Experimental study
24 design and subject recruitment were performed by SG, HAG, AGS, MGP, JF and RdeS. Gait
25 experiments and statistical analyses of the data were undertaken by SG, HAG, and AGS. All
26 authors discussed and agreed on results and potential implications. The manuscript was initially
27 prepared by SG, HAG, AGS and MGP, but all authors contributed substantially to its revision
28 and final form and approved the final submitted manuscript.

29

30 **Conflict of interest statement.** All authors declare no conflict of interest.

31 **ABSTRACT**

32 No data are available to describe six-degree-of-freedom (6-DOF) knee-joint kinematics for one
33 complete cycle of overground walking subsequent to total knee arthroplasty (TKA). The aims of
34 this study were firstly, to measure 6-DOF knee-joint kinematics and condylar motion for
35 overground walking following TKA; and secondly, to determine whether such data differed
36 between overground and treadmill gait when participants walked at the same speed during both
37 tasks. A unique mobile biplane X-ray imaging system enabled accurate measurement of 6-DOF
38 TKA knee kinematics during overground walking by simultaneously tracking and imaging the
39 joint. The largest rotations occurred for flexion-extension and internal-external rotation whereas
40 the largest translations were associated with joint distraction and anterior-posterior drawer.
41 Strong associations were found between flexion-extension and adduction-abduction ($R^2 = 0.92$),
42 joint distraction ($R^2 = 1.00$), and anterior-posterior translation ($R^2 = 0.77$), providing evidence of
43 kinematic coupling in the TKA knee. Although the measured kinematic profiles for overground
44 walking were grossly similar to those for treadmill walking, several statistically significant
45 differences were observed between the two conditions with respect to temporo-spatial
46 parameters, 6-DOF knee-joint kinematics, and condylar contact locations and sliding. Thus,
47 caution is advised when making recommendations regarding knee implant performance based on
48 treadmill-measured knee-joint kinematic data.

49

50 **Keywords:** Gait, joint replacement, implant wear, biplane X-ray fluoroscopy, knee model, joint
51 loading

52

53

54

INTRODUCTION

55 The ability to accurately measure in vivo knee-joint kinematics subsequent to total knee
56 arthroplasty (TKA) is important for determining joint-contact loading at the knee, predicting
57 implant component wear, and evaluating the effects of implant design and surgical technique on
58 TKA performance. Biplane X-ray fluoroscopy is currently the most accurate non-invasive
59 method available for measuring dynamic joint motion with mean errors of 0.29 mm for
60 translations and 0.25° for rotations reported for in vivo measurements of knee-joint kinematics
61 following TKA¹. There are, however, limitations associated with this method. Because the two
62 sets of X-ray sources and image intensifiers represent a combined mass of up to 150 kg, current
63 systems are designed to remain stationary during operation. Furthermore, the image capture
64 volume is defined by the intersection of two cone-shaped X-ray beams, and is therefore
65 relatively small (i.e., the base diameter and height of each cone beam are typically 300 mm and
66 1000 mm, respectively). Thus, studies which have used biplane fluoroscopy to record knee-joint
67 kinematics during walking have had to use a treadmill and have been unable to generate data for
68 an entire gait cycle²⁻⁵.

69

70 In vivo knee-joint kinematics for treadmill walking may not be identical with those for
71 overground walking. Evidence to support this assertion is available from some skin-marker-
72 based motion capture studies that have observed differences in knee-joint kinematic data for
73 healthy people when comparing treadmill and overground walking⁶⁻⁸. Understanding whether or
74 not differences exist between treadmill and overground walking for in vivo knee-joint kinematics
75 in people following TKA is important, as mathematical models used to predict TKA wear
76 patterns are sensitive to imported knee-joint kinematic data^{9,10}.

77

78 In the present study, a unique Mobile Biplane X-ray (MoBiX) imaging system enabled accurate
79 measurement of TKA knee-joint kinematics during overground walking by simultaneously
80 tracking and imaging the joint. The MoBiX system is capable of measuring six-degree-of-
81 freedom (6-DOF) TKA knee-joint kinematics during overground walking with maximum RMS
82 errors of 0.33 mm for translations and 0.65° for rotations¹¹. Our specific aims were firstly, to
83 describe in vivo 6-DOF knee-joint kinematics and condylar motion subsequent to TKA for one
84 complete cycle of overground walking; and secondly, to determine whether such data differed
85 between overground and treadmill gait when participants walked at the same speed during both
86 tasks.

87

88

METHODS

89 **Design:** One-way repeated measures

90 **Level of Evidence:** III

91 **Participants**

92 Ten people (5 females and 5 males; age, 69 ± 6 yrs; height, 166 ± 7 cm; weight, 88 ± 10 kg) with
93 unilateral TKA were recruited to this study. All participants had undergone surgery (Genesis II
94 posterior-stabilized total knee replacement, Smith & Nephew Inc., Memphis, TN, USA) at least
95 15 months (mean 25 ± 7 months) prior to testing. Approval for the study was obtained from the
96 Human Research Ethics Committee at The University of Melbourne (ID# 1033086) and each
97 participant gave informed consent prior to data collection.

98

99

100 **Gait experiments**

101 6-DOF knee-joint kinematics were measured for one complete gait cycle using the MoBiX
102 imaging system (Figure 1)¹¹, which tracked and imaged the knee at 200 Hz with an image
103 resolution of 1024×1024 pixels. The fluoroscopy units on the MoBiX system were set to
104 continuous mode with 110 kV and 13.1 mA. Each participant was exposed to X-ray radiation for
105 no more than 25 seconds for the entire experiment, hence the maximum exposure estimated for
106 each participant was 0.1 mSv. Full-body three-dimensional joint motion data were recorded
107 synchronously with the X-ray images using a 9-camera video-based motion capture system
108 (VICON Motion Systems Ltd., UK) sampling at a rate of 120 Hz. For the overground walking
109 trials, all three components of the ground reaction force (GRF) were recorded using two portable
110 strain-gauged force plates (AMTI Accugait, Watertown, MA) mounted flush with a 4.8 m long
111 wooden walkway and sampling at 1,080 Hz (Figure 1).

112

113 Participants were instructed to attend the Biomotion Laboratory at The University of Melbourne
114 on two separate occasions. The first session took approximately one hour and involved
115 familiarizing participants with the experimental protocol and equipment. Participants practiced
116 walking over ground and on a treadmill alongside the MoBiX imaging system until they were
117 comfortable with each task. The second session took approximately 3.5 hours and involved
118 experimental data collection, which took place no more than 1 week after the initial
119 familiarization session.

120

121 During data collection each participant wore shorts, a sleeveless lead vest and sandals (Nike
122 Straprunner IV, Beaverton, Oregon). Retro-reflective markers were placed on the participant's

123 skin following a previously described approach¹². All participants completed the overground
124 walking trials prior to treadmill walking to ensure walking speeds between the two conditions
125 were matched as closely as possible. The participant was provided with ~10 minutes to practice
126 walking over ground on the wooden walkway, initially without but then with the MoBiX system
127 tracking their implanted knee. Once the participant was comfortable with the testing procedure,
128 they performed two separate overground walking trials at a self-selected speed during which
129 biplane X-ray images of the implanted knee, full-body motion, and GRF data were recorded
130 simultaneously for an entire gait cycle. Overground walking speed was estimated from the
131 average speed of a retro-reflective marker mounted on the posterior aspect of the pelvis over the
132 second sacral spinous process. Next, the wooden walkway and force plates were removed and a
133 treadmill (T9350, Vision Fitness, Morwell VIC) was positioned in the middle of the
134 measurement zone. The participant practiced walking on the treadmill for approximately 3
135 minutes at a speed matched to their overground walking speed. Participants were permitted to
136 hold onto the handrails of the treadmill if they felt insecure. Once the participant indicated they
137 were comfortable walking on the treadmill whilst being tracked by the MoBiX system, biplane
138 X-ray images and full-body motion data were collected simultaneously for two complete cycles
139 of treadmill walking.

140

141 **Data Analysis**

142 Heel-strike and toe-off were identified using the trajectories of markers mounted on the posterior
143 aspect of the heel and the dorsal aspect of the first toe, respectively. GRF data recorded for
144 overground walking were used to determine the specific features in these marker trajectories

145 associated with heel-strike and toe-off. Several temporo-spatial parameters were then determined
146 based upon these events, including stride time, stride length, cadence, stance time, swing time,
147 and stance/swing ratio.

148
149 6-DOF joint motion for the implanted knee was determined from the biplane X-ray images using
150 a procedure (described in detail elsewhere¹¹) that combined an open-source software program
151 called JointTrack¹³ with a custom image processing and pose-estimation program developed in
152 MATLAB (The Mathworks Inc., Natick, MA). A joint coordinate system convention¹⁴ was used
153 to describe 6-DOF knee-joint motion with respect to anatomically meaningful axes (Figure 2).
154 Joint kinematic measurements were filtered using a Butterworth filter with a cut-off frequency of
155 20 Hz.

156
157 The positions of the contact centers in the medial and lateral compartments were calculated for
158 201 time steps over the gait cycle. To approximate the position of the contact center, the point on
159 the femoral condyle closest to the tibial tray was used for each compartment⁹. The anterior-
160 posterior and medial-lateral positions of the contact center on the tibial bearing as well as the
161 sliding distance and velocity between the femoral component and the tibial bearing were
162 determined for the 201 time steps for each compartment. The total sliding distance (TSD) in each
163 compartment was calculated as the sum of the magnitudes of the sliding distances between the
164 femoral component and tibial bearing over one gait cycle. The absolute sliding velocity (ASV)
165 was calculated as the instantaneous velocity of the contact center on the femoral component
166 relative to the tibial bearing at each time step. The mean ASV for each compartment was

167 calculated by finding the mean of the absolute values of the sliding velocity at each time step
168 over one gait cycle.

169

170 The coefficient of determination (R^2) was used to quantify the degree of association between
171 knee flexion and the remaining five DOFs of knee-joint motion for overground walking.

172 Overground and treadmill walking were compared using various outcome measures, including
173 temporo-spatial parameters, discrete knee-joint kinematic parameters, TSD and mean ASV.

174 Student's paired t-test was used to compare these parameters for the two walking conditions, and
175 differences were considered statistically significant when $p < 0.05$.

176

177

RESULTS

178 **Overground walking**

179 The mean self-selected overground walking speed for the participants was 0.93 ± 0.12 m/s. The
180 largest rotational motion was flexion-extension, followed by internal-external rotation and
181 adduction-abduction (Figure 3). The knee was fully extended at heel-strike and then flexed in
182 early stance, reaching a peak flexion angle of 4.2° at contralateral toe-off. It then extended until
183 just prior to contralateral heel-strike, before flexing again in preparation for swing. The knee
184 continued to flex during early swing and then extended fully prior to heel-strike. Peak flexion
185 angle during swing was 53.2° and occurred at 72.5% of the gait cycle. The tibia was externally
186 rotated by 0.9° at heel-strike and continued to rotate externally during loading response before
187 reaching a peak angle of 3.2° near contralateral toe-off. External rotation then decreased and the
188 tibia began to internally rotate. Peak internal rotation of 2.4° occurred at contralateral heel-strike.
189 Internal rotation then decreased and the tibia moved into external rotation just before toe-off.

190 External rotation increased gradually during swing, peaked, and then decreased in terminal
191 swing. The mean knee abduction angle was 0.1° at heel-strike and remained more-or-less
192 constant until mid-stance (~40% of the gait cycle). The knee then adducted until mid-swing
193 (~75.5% of the gait cycle), where it peaked at 2.5° before decreasing to 0.1° in terminal swing.
194 Flexion-extension and adduction-abduction were strongly associated ($R^2 = 0.92$), whereas
195 flexion-extension and internal-external rotation were not ($R^2 = 0.03$).

196

197 The largest translational motion during overground walking was joint distraction, followed by
198 anterior drawer and lateral shift (Figure 3). At heel-strike, mean joint distraction was 8.2 mm,
199 which increased slightly during loading response before reaching a peak of 9.6 mm at
200 contralateral toe-off. Joint distraction then began to increase just prior to contralateral heel-strike,
201 reaching a peak value of 25.5 mm during swing (~72.5% of gait cycle). The tibia was located 7.8
202 mm posterior to the femur at heel-strike, before moving posteriorly by 1.2 mm during loading
203 response and translating anteriorly by 0.9 mm during single leg support. The tibia then translated
204 posteriorly after contralateral heel-strike during the second period of double support. Peak
205 posterior translation during the second period of double support was 16.0 mm and occurred just
206 prior to toe-off, whereas peak posterior translation during swing was slightly greater at 18.0 mm.
207 Total medial-lateral shift was small (1.6 mm). At heel-strike, mean lateral shift was 0.0 mm and
208 varied very little (0.5 mm) during the first half of the gait cycle. The tibia shifted medially at toe-
209 off, then laterally during initial swing, and gradually returned to the neutral position prior to
210 heel-strike. Flexion-extension correlated precisely with joint distraction ($R^2 = 1.00$) and was also
211 strongly associated with anterior-posterior translation ($R^2 = 0.77$), but less so with medial-lateral
212 shift ($R^2 = 0.39$).

213
214 The tibiofemoral contact centers shifted more in the anterior-posterior direction than in the
215 medial-lateral and proximal-distal directions during overground walking (Figures 4 and 5). Both
216 the medial and lateral compartment contact centers had similar patterns of anterior-posterior
217 movement throughout the gait cycle, except for early stance where the medial compartment
218 contact center was more posterior compared to the lateral compartment contact center. At heel-
219 strike the medial and lateral compartment contact centers were located at mean distances of 4.2
220 mm and 3.3 mm posterior to the tibial origin, respectively. Both contact centers then shifted a
221 little further posteriorly during loading response to reach 7.3 mm (medial) and 5.4 mm (lateral).
222 After contralateral toe-off both contact centers moved anteriorly and then began moving
223 posteriorly again subsequent to mid-stance. Anterior translation peaked just prior to toe-off and
224 twice during swing. The maximum displacements of the contact centers in the anterior-posterior
225 direction were 6.4 mm and 4.1 mm in the medial and lateral compartments, respectively. The
226 medial and lateral compartment contact centers had identical patterns of movement in the
227 medial-lateral direction throughout the gait cycle. The contact centers remained almost at a fixed
228 medial-lateral position during most of the stance phase. During terminal stance, the contact
229 centers shifted laterally to a peak lateral position at toe-off, then shifted medially reaching a peak
230 medial position during early swing, and finally shifted laterally again prior to heel-strike. The
231 maximum displacement of the contact centers in the medial-lateral direction was ~2 mm. The
232 contact centers on the femoral component remained relatively fixed in the proximal-distal
233 direction with respect to the tibia for the entire gait cycle. The medial contact center moved
234 distally during late stance and proximally at toe off while the lateral contact center moved

235 proximally during early swing. Nonetheless, peak-to-peak proximal-distal translations remained
236 < 1 mm (Figure 5).

237

238 **Overground versus treadmill walking**

239 Four participants walked on the treadmill without using the handrails, while the remaining six
240 placed their fingers lightly on the handrails during ambulation. Stride time, stride length,
241 stance/swing ratio and stance time were all significantly reduced for treadmill compared to
242 overground walking whereas cadence was significantly higher for treadmill walking (Table 1).

243

244 Overall, the gross patterns of rotational and translational motions of the knee were similar for
245 overground and treadmill walking (Figure 3), although several discrete parameters displayed
246 statistically significant differences (Table 2). Significant differences occurred mainly in the
247 sagittal plane for flexion-extension, anterior-posterior drawer and joint distraction (Figure 3 and
248 Table 2). The magnitudes of the differences between treadmill and overground walking for all
249 other DOF's were less than 0.5 mm and 1° (Figure 3) for translations and rotations, respectively.
250 Peak knee flexion angle during swing was 3.1° larger ($p=0.04$) and that at heel-strike was 6.5°
251 larger ($p=0.03$) for treadmill walking compared to overground walking. Similarly, peak joint
252 distraction during swing was 1.3 mm larger ($p=0.01$) and joint distraction at heel-strike was 1.8
253 mm larger ($p=0.049$) for treadmill walking. Differences between treadmill and overground
254 walking were also evident in the profiles for anterior drawer during the first half of the gait cycle,
255 where anterior-posterior translation remained almost constant in overground walking whereas the
256 tibia translated anteriorly by ~4 mm in treadmill walking (Figure 3).

257

258 Subtle differences between treadmill and overground walking were observed in the anterior-
259 posterior, medial-lateral, and proximal-distal positions of the contact centers for both the medial
260 and lateral compartments, with differences being more pronounced in the anterior-posterior
261 direction (Figures 4 and 5). During early stance the contact center in the medial compartment
262 was located more anteriorly for treadmill walking compared to overground walking, whereas
263 during late swing the contact centers in both the medial and lateral compartments were located
264 more anteriorly for treadmill walking compared to overground walking (Figure 5). Sliding
265 velocity in both compartments peaked during late stance and late swing for both treadmill and
266 overground walking (Figure 6). Sliding velocities were higher in both compartments during late
267 stance and lower during late swing for treadmill walking compared to overground walking.
268 However, differences between the two conditions for TSD and mean ASV over one gait cycle in
269 both compartments were not statistically significant (Table 3).

270

271

DISCUSSION

272 We used mobile biplane X-ray imaging to noninvasively measure 6-DOF knee-joint kinematics
273 and condylar motion in 10 people following TKA for one cycle of overground walking. The
274 largest angular displacements occurred for flexion-extension and internal-external rotation
275 whereas the largest translations occurred for joint distraction and anterior-posterior drawer
276 (Figure 3). Strong associations were found between flexion-extension and several secondary
277 joint movements, specifically, adduction-abduction ($R^2 = 0.92$), joint distraction ($R^2 = 1.00$) and
278 anterior-posterior translation ($R^2 = 0.77$), providing evidence of kinematic coupling in the TKA
279 knee during overground gait. In the same 10 people, we also measured 6-DOF knee-joint
280 kinematics for one cycle of treadmill walking at a speed matched to their self-selected

281 overground speed. Whilst the general patterns of 6-DOF knee-joint kinematics and condylar
282 motions were similar between treadmill and overground walking (Figures 2-4), some clear
283 disparities in kinematic behavior were evident between the two conditions (Table 2). For
284 example, the tibia translated anteriorly relative to the femur for the majority of stance during
285 treadmill walking whereas minimal anterior-posterior translation occurred during the same
286 period of overground walking (Figure 3). Overall, our results show that 6-DOF kinematics and
287 condylar motion at the knee during treadmill walking are not identical with that which occurs
288 during overground walking.

289
290 How do 6-DOF knee-joint kinematic data for walking in people following TKA compare to
291 equivalent data in people with healthy knees? Lafortune et al.¹⁵ used intra-cortical pins to
292 measure 6-DOF knee-joint kinematics in five healthy young people for one complete cycle of
293 overground walking at a speed of 1.2 m/s. Our data for knee flexion-extension, anterior-posterior
294 translation and joint distraction for overground walking are consistent with their results.
295 However, differences exist for medial-lateral shift and internal-external rotation, suggesting that
296 these two kinematic DOF's are most sensitive to TKA. Our data for knee adduction-abduction
297 are also substantially different from that reported by Lafortune et al.¹⁵. Whilst we found the knee
298 to adduct during swing, these authors reported a contrary pattern of abduction, which may be
299 explained by differences in the bone coordinate systems used. Using a similar measurement
300 approach to the present study, Kozanek et al.³ recorded 6-DOF knee-joint kinematics via biplane
301 fluoroscopy in 8 healthy young adults for the stance phase of treadmill walking at a speed of 0.67
302 m/s. The patterns of knee flexion-extension and internal-external rotation found in the present
303 study are similar to those of Kozanek et al.³. However, the pattern of anterior-posterior

304 translation reported by these authors differs somewhat from that obtained for treadmill walking
305 in the current study. Our results indicate that the tibia translates anteriorly relative to the femur
306 between heel-strike and contralateral heel-strike, whereas Kozanek et al.³ found the tibia to
307 translate posteriorly and then anteriorly during early stance and to remain nearly constant
308 thereafter until contralateral heel-strike. These differences are likely due to the absence of the
309 cruciate ligaments in the knees of our participants who had all undergone posterior-stabilized
310 TKA surgery. Kozanek et al.³ also reported a joint distraction of ~2 mm for the intact knee
311 during stance compared to ~13 mm in the present study. This difference may be explained by the
312 different coordinate systems selected for the femur. Kozanek et al.³ located the origin of the
313 femur on the transepicondylar axis, which is close to the geometric axis of the condyles, whereas
314 the origin of the femur in the present study was chosen in accordance with methods established
315 by Grood and Suntay¹⁴ and was located more distally on the femur (Figure 2).

316

317 Joint distraction calculated in the present study represents the distance between the femoral and
318 tibial origins measured along the Z-axis of the tibia (Figure 2) and should not be interpreted as a
319 measure of the tibia separating from the femur. We note, however, that the tibiofemoral contact
320 points on the medial and lateral condyles of the femur moved less than 1 mm along the Z-axis of
321 the tibia for the duration of the gait cycle (Figure 5).

322

323 Our results regarding differences between treadmill and overground walking are consistent with
324 previous studies that compared knee kinematics calculated from motion capture data in healthy
325 age-matched individuals. Watt et al.⁸ found cadence increased by 6.78 steps/min and stride
326 length decreased by 0.09 m for treadmill compared to overground walking. Our results indicate

327 similar differences for the two conditions with an increase in cadence by 8.78 steps/min and a
328 decrease in stride length by 0.10 m for treadmill compared to overground walking. Our
329 participants also displayed reduced stance time but kept swing time almost unchanged for
330 treadmill compared to overground walking. This resulted in a reduced stance-to-swing ratio of
331 0.12 for treadmill walking, which is consistent with Parvataneni et al.⁶ who reported a reduction
332 of 0.13. Wass et al.¹⁶ reported that the knee flexion angle at heel-strike increased by 4.1° for
333 treadmill compared to overground walking, which is similar to the increase of 6.6° found here.

334

335 Several factors may have contributed to the differences in knee-joint kinematics between
336 overground and treadmill walking observed in the present study. The TKA patients may have
337 increased their cadence during treadmill walking in an attempt to gain better balance control on
338 the moving belt. Alternatively, the limited length of the treadmill may have had a psychological
339 effect on the participants who tried to avoid reaching the end of the treadmill belt by using a
340 shorter stride length, and hence a faster cadence. Increased knee flexion at heel-strike has been
341 reported as a strategy adopted for coping with the uncertainty involved in running on an irregular
342 surface¹⁷. A slightly bent knee at heel-strike reduces the effective mass and allows for better
343 shock attenuation, which may also reduce the potential for injury^{17, 18}. Perhaps our participants
344 flexed their knees more at heel-strike during treadmill walking to cope with the uncertainty
345 associated with an unfamiliar activity. One of the most noticeable differences in knee kinematics
346 between treadmill and overground walking was related to anterior drawer at heel-strike, with the
347 tibia positioned more posteriorly relative to the femur during treadmill walking compared to
348 overground walking (Figure 3). We speculate that for treadmill walking, the hamstring muscle
349 generates a larger force during terminal swing to maintain a more flexed knee at heel-strike. The

350 increased hamstring force pulls back on the proximal tibia causing the tibia to translate
351 posteriorly. This result is consistent with the increased activation of the biceps femoris during
352 terminal swing reported for treadmill walking¹⁹.

353

354 Flexion-extension, anterior-posterior translation and internal-external rotation have been reported
355 as the main contributors to implant wear²⁰. Whilst profiles for internal-external rotation were
356 similar for overground and treadmill walking, increases in knee flexion and anterior-posterior
357 translation and a reduction in stride time for treadmill walking collectively contributed to an
358 increase in sliding velocity, especially during late stance (Figure 6). This increased sliding
359 velocity together with relatively high joint contact loads during late stance may be particularly
360 relevant to calculations of implant wear as mathematical models used to predict tibial bearing
361 wear have relied on knee-joint kinematics measured during treadmill walking¹⁰. Further research
362 is needed to establish whether wear patterns are indeed different between treadmill and
363 overground walking.

364

365 The present study is not without limitations. First, the MoBiX imaging system moving alongside
366 the participants may have intimidated and hence adversely affected the participants' natural gait.
367 We gave each participant the opportunity to practice overground and treadmill walking with the
368 mobile gantry mechanism in operation, both during the familiarization session and again during
369 the test session immediately prior to data collection. Data were collected only after each
370 participant gave verbal confirmation that they were comfortable with the equipment and
371 experimental protocol. Because the MoBiX system tracked and imaged the participants' knees

372 during both overground and treadmill walking, it is unlikely that this factor contributed to the
373 observed differences in knee kinematics between the two walking conditions.

374

375 Second, six of the participants in the present study could not reproduce arm swing during
376 treadmill walking as they elected to use the handrail for additional support. A study on
377 familiarization to treadmill walking in unimpaired older people (aged 67 to 80) revealed that
378 more participants were able to walk without the use of handrails as familiarization increased¹⁶.
379 However, even after 14 minutes of familiarization only five participants out of 16 were able to
380 walk without the use of handrails and two of the participants could not complete the task due to
381 fatigue and requested that the treadmill be stopped at 7 minutes and 10 minutes¹⁶. Thus, in the
382 current study more subjects may have been able to walk without the use of the handrails had
383 more time been allocated for familiarization to treadmill walking. Nevertheless, we did provide
384 participants with familiarization periods comparable to those reported in the literature. Varying
385 lengths of treadmill familiarization times have been reported, including 30 seconds⁴, at least 2
386 minutes⁸, 3 minutes²¹, 2 to 4 minutes⁶ and 14 minutes¹⁶. Our participants undertook one
387 familiarization session and had a total practice time of at least 7 minutes on the treadmill prior to
388 data collection. We therefore suggest that this duration was appropriate because we were able to
389 collect data before participants became fatigued and also because it is longer than the durations
390 employed by many previous studies.

391

392 Third, the results of the present study are based on one particular design of posterior-stabilized
393 TKAs. Nevertheless, our findings are consistent with other studies measuring differences in
394 temporo-spatial parameters and knee-joint angles between overground and treadmill walking for

395 healthy elderly subjects^{6, 8}. This may be an indication that the locations of tibiofemoral contact
396 and other kinematic parameters at the knee are different for overground and treadmill walking in
397 healthy older subjects and perhaps in patients with other TKA designs as well. Further research
398 is needed to better understand these issues.

399
400 In summary, the results of this study yield accurate measurements of 6-DOF knee-joint
401 kinematics and condylar motion for one complete cycle of overground TKA gait. Although the
402 measured kinematic profiles for overground walking were grossly similar to those for treadmill
403 walking, several statistically significant differences were observed between the two conditions
404 with respect to temporo-spatial parameters, 6-DOF knee-joint kinematics, and tibiofemoral joint
405 contact center motion. Thus, caution is advised when making recommendations regarding TKA
406 performance based on treadmill-measured knee-joint kinematic data.

407

408

ACKNOWLEDGMENTS

409 This study was funded in part by an Australian Research Council Linkage Projects Grant
410 (LP0990369) and an Innovation Fellowship from the Victorian Endowment for Science,
411 Knowledge and Innovation provided to MGP. We thank Smith & Nephew Inc. for providing the
412 geometric models of the knee implants used for pose-estimation.

413

Author Manuscript

414

REFERENCES

- 415 1. Bingham J, Li G. 2006 An optimized image matching method for determining in-vivo
416 TKA kinematics with a dual-orthogonal fluoroscopic imaging system. *J Biomech Eng.*
417 128: 588-595.
- 418 2. Anderst W, Zael R, Bishop J, et al. 2009 Validation of three-dimensional model-based
419 tibio-femoral tracking during running. *Med Eng Phys.* 31: 10-16.
- 420 3. Kozanek M, Hosseini A, Liu F, et al. 2009 Tibiofemoral kinematics and condylar motion
421 during the stance phase of gait. *J Biomech.* 42: 1877-1884.
- 422 4. Li G, Kozanek M, Hosseini A, et al. 2009 New fluoroscopic imaging technique for
423 investigation of 6DOF knee kinematics during treadmill gait. *J Orthop Surg.* 4: 6.
- 424 5. Tashman S, Kolowich P, Collon D, et al. 2007 Dynamic function of the ACL-
425 reconstructed knee during running. *Clin Orthop.* 454: 66-73.
- 426 6. Parvataneni K, Ploeg L, Olney SJ, Brouwer B. 2009 Kinematic, kinetic and metabolic
427 parameters of treadmill versus overground walking in healthy older adults. *Clin Biomech.*
428 24: 95-100.
- 429 7. Riley PO, Paolini G, Della Croce U, et al. 2007 A kinematic and kinetic comparison of
430 overground and treadmill walking in healthy subjects. *Gait Posture.* 26: 17-24.

- 431 8. Watt JR, Franz JR, Jackson K, et al. 2010 A three-dimensional kinematic and kinetic
432 comparison of overground and treadmill walking in healthy elderly subjects. Clin
433 Biomech. 25: 444-449.
- 434 9. DesJardins JD, Banks SA, Benson LC, et al. 2007 A direct comparison of patient and
435 force-controlled simulator total knee replacement kinematics. J Biomech. 40: 3458-3466.
- 436 10. Fregly BJ, Sawyer WG, Harman MK, Banks SA. 2005 Computational wear prediction of
437 a total knee replacement from in vivo kinematics. J Biomech. 38: 305-314.
- 438 11. Guan S, Gray HA, Keynejad F, Pandy MG. 2016 Mobile biplane X-ray imaging system
439 for measuring 3D dynamic joint motion during overground gait. IEEE Trans Med
440 Imaging. 35: 326-336.
- 441 12. Lai A, Lichtwark GA, Schache AG, et al. 2015 In vivo behavior of the human soleus
442 muscle with increasing walking and running speeds. J Appl Physiol. 118: 1266-1275.
- 443 13. Mu S, JointTrack: An open-source, easily expandable program for skeletal kinematic
444 measurement using model-image registration., in Department of Mechanical and
445 Aerospace Engineering. 2007, University of Florida: Gainesville, Florida, USA.
- 446 14. Grood ES, Suntay WJ. 1983 A joint coordinate system for the clinical description of
447 three-dimensional motions: application to the knee. J Biomech Eng. 105: 136-144.
- 448 15. Lafortune MA, Cavanagh PR, Sommer HJ, Kalenak A. 1992 Three-dimensional
449 kinematics of the human knee during walking. J Biomech. 25: 347-357.

- 450 16. Wass E, Taylor NF, Matsas A. 2005 Familiarisation to treadmill walking in unimpaired
451 older people. *Gait Posture*. 21: 72-79.
- 452 17. Thomas JM, Derrick TR. 2003 Effects of step uncertainty on impact peaks, shock
453 attenuation, and knee/subtalar synchrony in treadmill running. *J Appl Biomech*. 19: 60-
454 70.
- 455 18. Miyazaki K. 1998 Impact loading on the foot and ankle and its attenuation during level
456 walking. *Kurume Med J*. 45: 75-80.
- 457 19. Arsenault AB, Winter DA, Marteniuk RG. 1986 Treadmill versus walkway locomotion in
458 humans: an EMG study. *Ergonomics*. 29: 665-676.
- 459 20. Fitzpatrick CK, Komistek RD, Rullkoetter PJ. 2014 Developing simulations to reproduce
460 in vivo fluoroscopy kinematics in total knee replacement patients. *J Biomech*. 47: 2398-
461 2405.
- 462 21. Lee SJ, Hidler J. 2008 Biomechanics of overground vs treadmill walking in healthy
463 individuals. *J Appl Physiol*. 104: 747-755.

464

465

466
467

TABLES

468 Table 1: Temporo-spatial gait parameters measured for treadmill and overground walking.
469 CHS, contralateral heel-strike.

	Overground ^a	Treadmill ^a	Difference ^a	P-value	Effect size
Walking speed (m/s)	0.93	0.93	-0.00	0.82	0.06
Stride time (s)	1.28	1.17	-0.11	0.00*	0.97
Cadence (steps/min)	95.11	103.90	8.78	0.00*	0.98
Stride length (m)	1.17	1.07	-0.10	0.00*	0.98
Stance/swing ratio	1.92	1.80	-0.12	0.01*	0.84
Stance time (s)	0.84	0.75	-0.09	0.00*	1.00
Swing time (s)	0.44	0.42	-0.02	0.08	0.42
CHS (% of gait cycle)	49.63	50.58	0.95	0.24	0.20

470 * Significant difference ($p < 0.05$)471 ^a Mean values across subjects.472
473

474 Table 2: Mean values of representative knee-joint kinematic parameters measured for treadmill
 475 and overground walking. 'Increment during single support' describes the increment in
 476 knee abduction angle at contralateral heel-strike compared to the value at contralateral
 477 toe-off.

		Overground ^a	Treadmill ^a	Difference ^a	P-value	Effect size
Anterior Drawer (mm)	Value at heel-strike	-7.84	-11.35	-3.52	0.00*	0.98
Joint Distraction (mm)	Value at heel-strike	8.15	9.97	1.81	0.05*	0.53
	Peak value during gait cycle	25.67	26.99	1.33	0.01*	0.88
Flexion (degree)	Value at heel-strike	-1.50	5.01	6.51	0.03*	0.63
	Peak value during gait cycle	53.84	56.95	3.11	0.04*	0.59
Abduction (degree)	Increment during single support	-0.26	0.20	0.46	0.01*	0.78

478 * Significant difference ($p < 0.05$)

479 ^a Mean values across subjects.

480

481

482 Table 3: Total sliding distance (TSD) and mean absolute sliding velocity (ASV) measured for
 483 treadmill and overground walking. All data are for one complete gait cycle.

Wear Parameter	Condyle	Overground ^a	Treadmill ^a	Increase ^a	P-value	Effect Size
TSD (mm)	Medial	68.77	67.98	-0.79 (-1%)	0.73	0.06
	Lateral	67.97	66.35	-1.62 (-2%)	0.38	0.13
Mean ASV (mm/s)	Medial	54.15	58.93	4.78 (9%)	0.07	0.45
	Lateral	53.77	57.27	3.49 (6%)	0.10	0.37

484 ^a Mean values across subjects

485

Author Manuscript

486
487**FIGURE LEGENDS**

488 Figure 1: Schematic diagram illustrating the experimental setup for the overground walking
489 trials. The mobile biplane X-ray (MoBiX) imaging system comprised of two
490 fluoroscopy units and a customized robotic gantry mechanism. The two X-ray tubes
491 and two image intensifiers were mounted on the robotic gantry and were moved along
492 the horizontal and vertical guides by horizontal and vertical servomotors, respectively.
493 A wooden walkway (dimensions 4.8 m x 0.6 m) was placed on the floor between the
494 two horizontal guides, and two force plates were mounted on the walkway as shown.
495 As the participant walked along the walkway, a high-speed digital camera imaged a
496 retroreflective marker located near the implanted knee, and these images were then
497 relayed to a real-time computer (not shown) that generated velocity commands which
498 controlled the motion of the X-ray units via the servomotors. Biplane X-ray images
499 were captured at 200 Hz for all trials. Nine high-speed VICON cameras (one camera
500 which was mounted on the ceiling is not shown) surrounding the MoBiX system were
501 operated at 120 Hz to record the trajectories of retro-reflective skin markers, while the
502 force plates sampled at 1,080 Hz and recorded all three components of the ground
503 reaction force. A synchronization light (Sync Light) was used to synchronize the
504 biplane X-ray image data with the video motion capture data. For the treadmill
505 walking trials, the wooden walkway was removed and a treadmill was placed on the
506 floor between the two horizontal guides of the gantry mechanism.

507

508 Figure 2: Coordinate systems defined for the femoral and tibial components of a left posterior-
509 stabilized total knee replacement. The origin of the femoral reference frame was
510 located at the posterior-most point on the mid-plane of the intercondylar notch. The Z-
511 axis (Z_F) was assumed to be perpendicular to the transverse flat surface of the femoral
512 component. The X-axis (X_F) was taken parallel to the posterior chamfer and
513 perpendicular to the Z-axis. The Y-axis (Y_F) was mutually perpendicular to the Z-axis
514 and X-axis. The Y-axis (Y_T) of the tibial component was assumed to be parallel to the
515 medial and lateral surfaces of the cam post and parallel to the tibial tray. The X-axis
516 (X_T) was taken parallel to the tibial tray and perpendicular to the Y-axis. The Z-axis
517 (Z_T) was mutually perpendicular to the X-axis and Y-axis. The origin of the tibial
518 reference frame was positioned at the center of the minimum bounding rectangle of the
519 tibial tray and offset proximally from the tibial tray by a distance equal to the nominal
520 thickness of the tibial bearing. X_F and Z_T were assumed to be body-fixed axes. The
521 floating axis (W) was defined as mutually perpendicular to the body-fixed axes (X_F
522 and Z_T), consistent with the definition given by Grood and Suntay¹⁴. Flexion (R_1),
523 abduction (R_2), and external rotation (R_3) were measured for the tibia about X_F , W ,
524 and Z_T . Lateral shift (T_1), anterior drawer (T_2), and joint distraction (T_3) were
525 measured as translations of the tibial origin relative to the femoral origin along X_F , W ,
526 and Z_T , respectively.

527

528

529 Figure 3: 6-DOF knee-joint kinematics measured for overground and treadmill walking. Positive
530 angular displacements of the tibia relative to the femur are described by flexion,

531 abduction, and external rotation (first row), while positive translations of the tibia
532 relative to the femur are described by lateral shift, anterior drawer, and joint distraction
533 (third row). TM-OG represents the difference in knee-joint rotations (second row) and
534 in knee-joint translations (fourth row) between treadmill (TM) and overground (OG)
535 walking. All curves represent mean data while the shaded areas represent ± 1 standard
536 deviation from the mean. Two trials of each task were analyzed for seven of the ten
537 participants. For the remaining three participants, one had only 1 overground trial and
538 1 treadmill trial; one participant had 1 overground trial and 2 treadmill trials; and one
539 participant had 2 overground trials and 4 treadmill trials. The vertical dotted lines
540 mark the following gait events: CTO – contralateral toe-off; CHS – contralateral heel-
541 strike; TO – toe-off; HS – heel-strike. Rotations and translations are described in an
542 established joint coordinate system¹⁴. Translations of the femur in the tibial reference
543 frame³ are given in the Supplementary Material (Figure S-1).

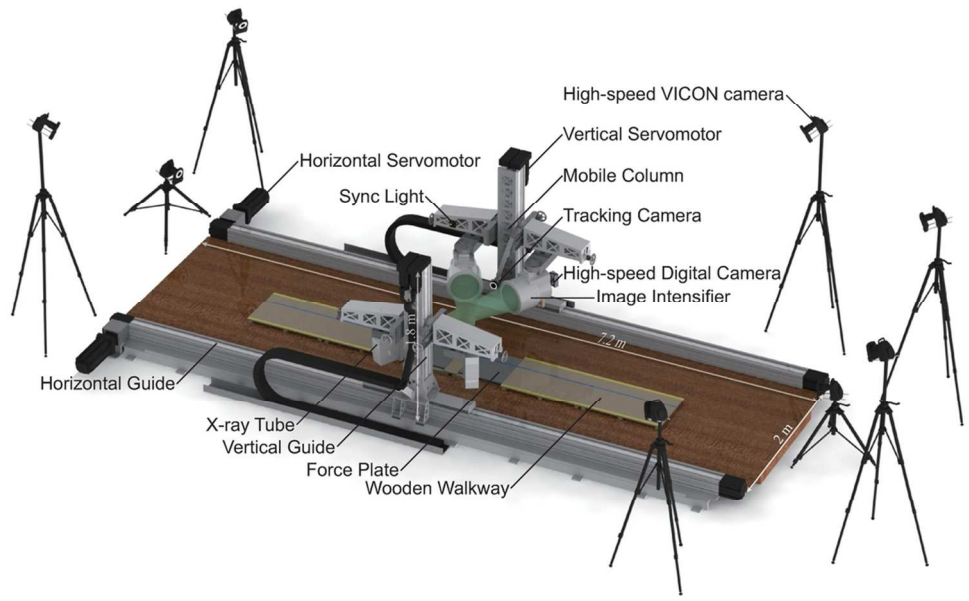
544
545 Figure 4: Mean trajectories of the tibiofemoral contact centers plotted on the top surface of the
546 tibial bearing for one cycle of both overground walking (OG) and treadmill walking
547 (TM). The tibial coordinate system is defined in Fig 2; scales used for the anterior-
548 posterior and medial-lateral axes are in millimeters. The insets show scaled-up views
549 of the contact center trajectories in the medial and lateral compartments. The red and
550 blue dots represent the mean positions of the contact centers calculated over one gait
551 cycle for treadmill and overground walking, respectively. The asterisks indicate
552 statistically significant ($p < 0.05$) differences in the positions of the mean contact
553 centers between overground and treadmill walking.

554

555 Figure 5: Mean anterior-posterior, medial-lateral, and proximal-distal positions of the contact
556 centers in the medial and lateral compartments of the tibiofemoral joint for one gait
557 cycle. Data shown are described in the tibial reference frame. Anterior, medial, and
558 proximal displacements are positive. All curves represent mean data while the shaded
559 areas represent ± 1 standard deviation from the mean.

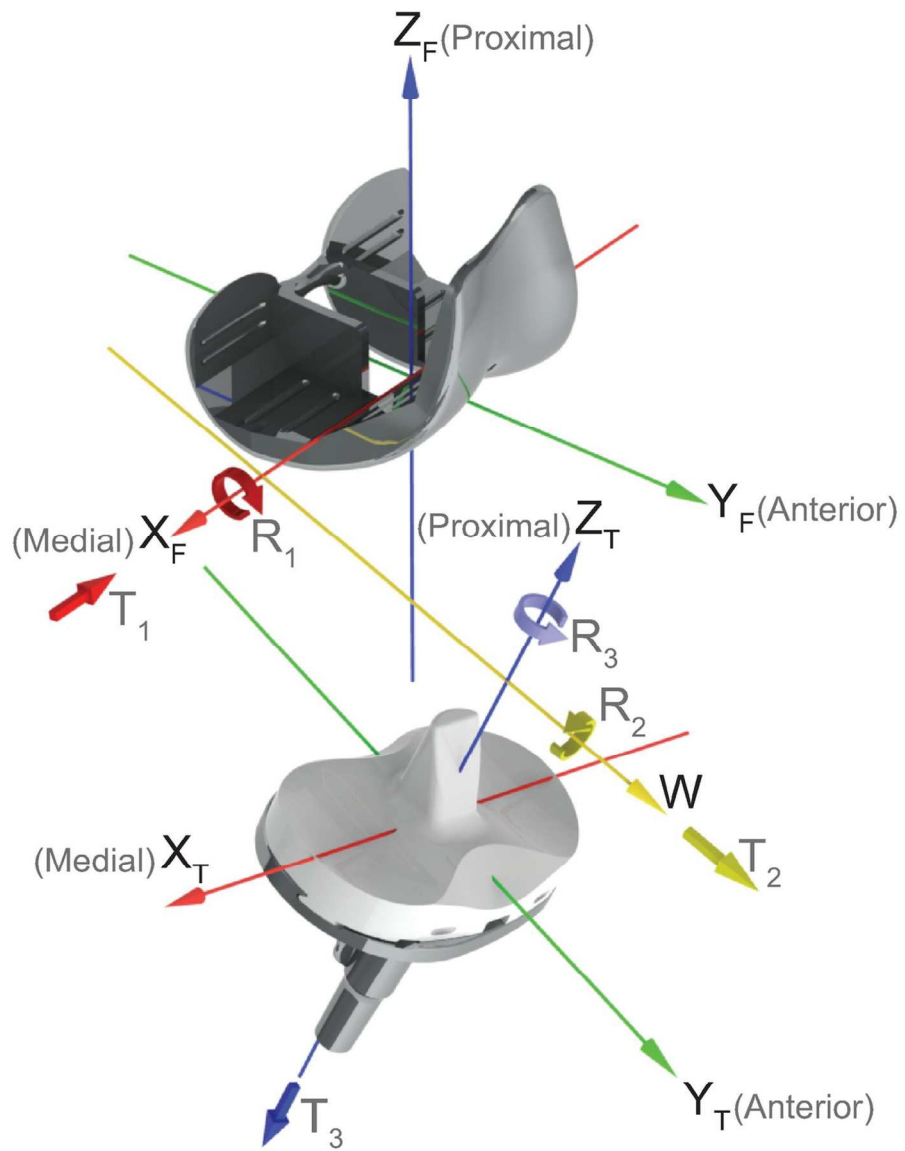
560

561 Figure 6: Absolute sliding velocity between the femoral component and the tibial bearing
562 plotted for one gait cycle. All curves represent mean data while the shaded areas
563 represent ± 1 standard deviation from the mean.



Caption is at the end of the document containing the main text
Figure 1
99x59mm (300 x 300 DPI)

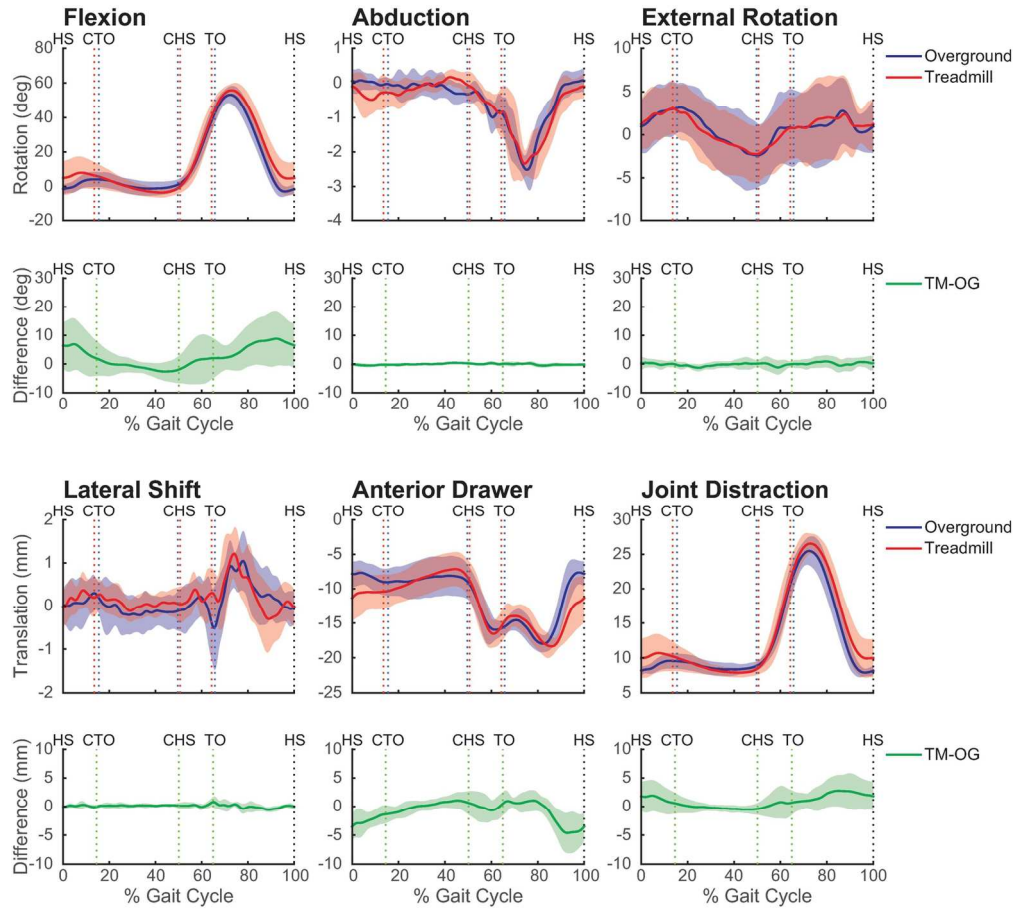
Author Manuscript



Caption is at the end of the document containing the main text

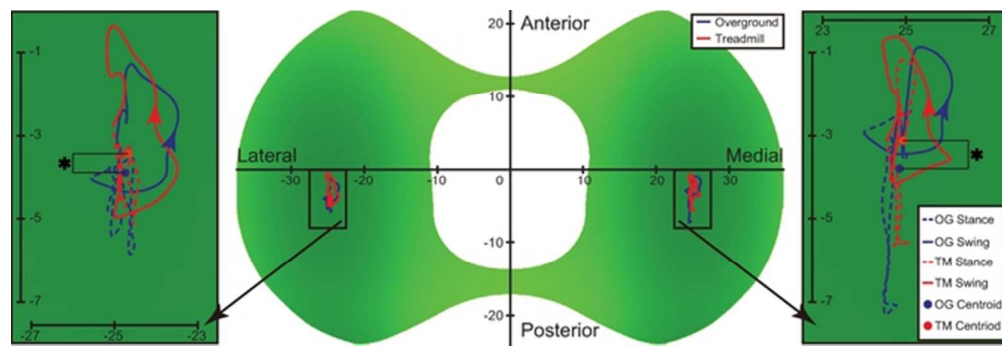
Figure 2

108x143mm (300 x 300 DPI)



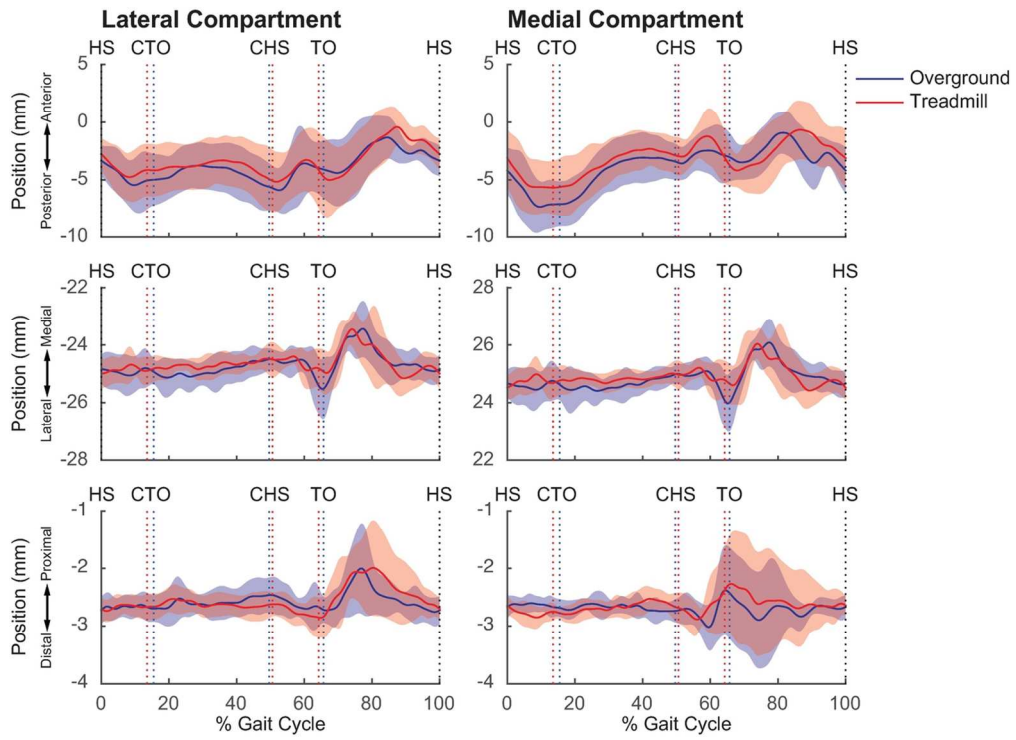
Caption is at the end of the document containing the main text
Figure 3
150x136mm (300 x 300 DPI)

Author



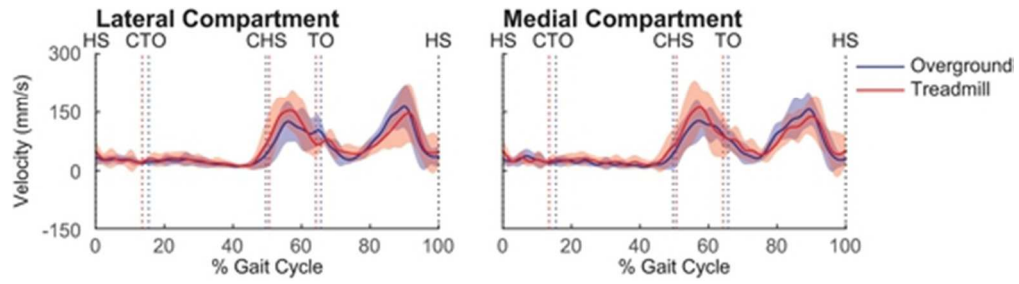
Caption is at the end of the document containing the main text
Figure 4
56x18mm (300 x 300 DPI)

Author Manuscript



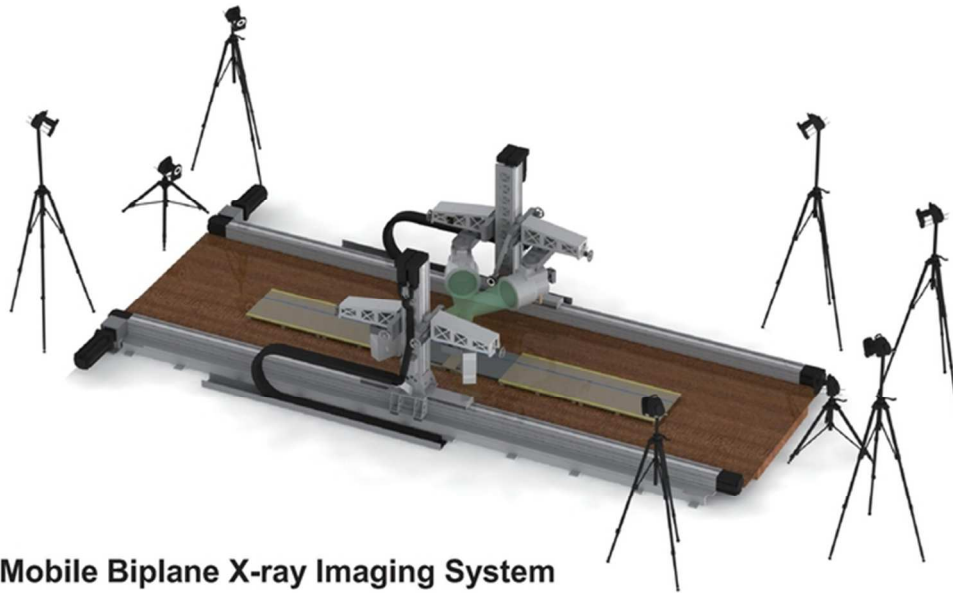
Caption is at the end of the document containing the main text
Figure 5
121x88mm (300 x 300 DPI)

Author Manuscript



Caption is at the end of the document containing the main text
Figure 6
45x12mm (300 x 300 DPI)

Author Manuscript

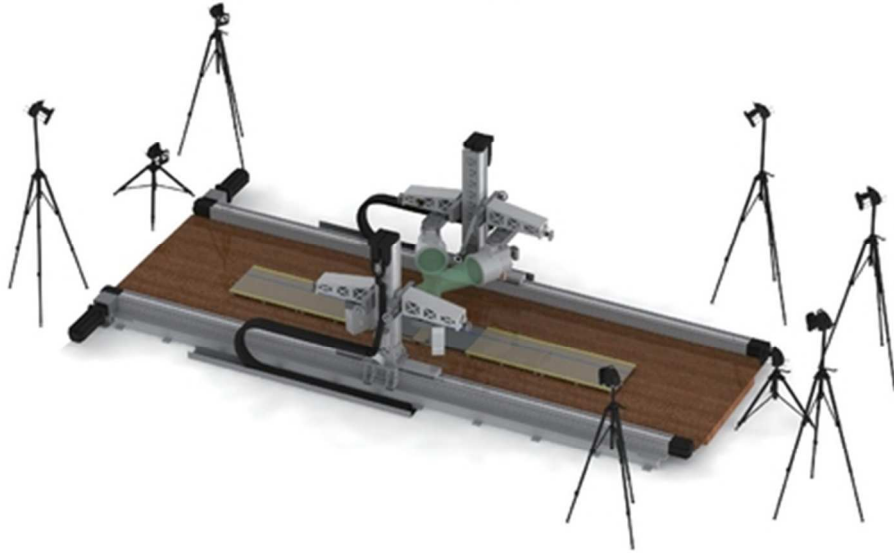


Mobile Biplane X-ray Imaging System

59x35mm (300 x 300 DPI)

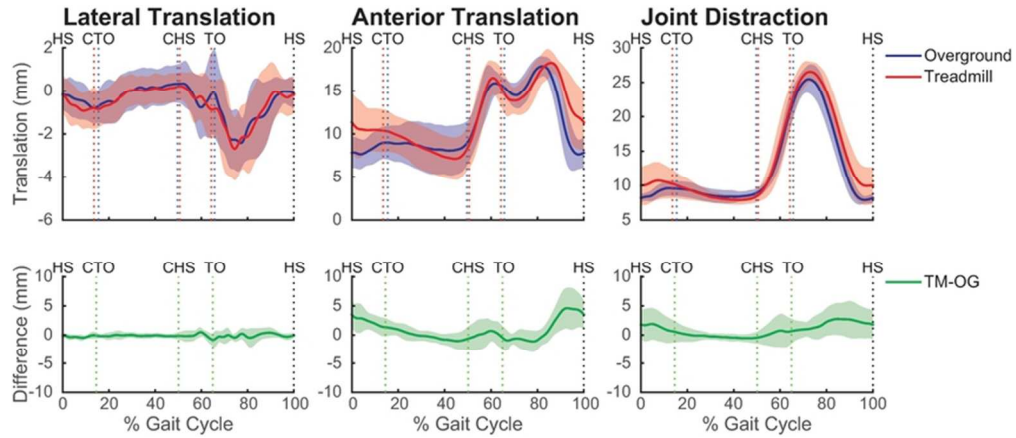
Author Manuscript

Mobile Biplane X-ray Imaging System



39x25mm (300 x 300 DPI)

Author Manuscript



The caption is in the document "TKA Kinematics_supplementary material_21October2016.doc"
Figure S-1
71x31mm (300 x 300 DPI)

Author Manuscript